

Weak charge-transfer complexes based on conjugated polymers for plastic solar cells

A.A. Bakulin^a, S.G. Elizarov^a, A.N. Khodarev^a, D.S. Martyanov^a,
I.V. Golovnin^a, D.Y. Paraschuk^{a,*}, M.M. Triebel^b, I.V. Tolstov^b,
E.L. Frankevich^b, S.A. Arnautov^c, E.M. Nechvolodova^c

^a *International Laser Center, Moscow State University, Moscow 119992, Russia*

^b *Institute of Energy Problems of Chemical Physics, Russian Academy of Sciences, Leninsky prospect 38/2, Moscow 119334, Russia*

^c *Semenov Institute of Chemical Physics, Russian Academy of Sciences, ul. Kosygina 4, Moscow 119991, Russia*

Received 30 April 2004; received in revised form 22 May 2004; accepted 23 May 2004

Abstract

As known for short conjugated molecules, the absorption band of a weak (Mulliken) charge-transfer complex (CTC) can be tuned in the region where both the donor and acceptor are transparent. This can be used for tailoring low-band gap absorbing materials to match the solar spectrum. We studied donor/acceptor blends of poly[2-methoxy-5-(2'-ethyl-hexyloxy)-1,4-phenylene vinylene] (MEH-PPV) with 2,4,7-trinitrofluorenone or 2,6-dinitroantraquinone by a number of optical and photoelectric methods. From optical and vibrational IR absorption spectra, we found that the donor/acceptor blends demonstrate noticeable ground-state interaction indicating CTC formation. The CTC is characterized by a long absorption tail extending to the near-IR region. The blends also show strong quenching of photoluminescence (PL) and a near-IR photoinduced absorption (PIA) band, indicating donor/acceptor charge-transfer. Essentially, this band appears for both visible and IR pump wavelengths. In addition, to probe the charge photogeneration mechanisms, a magnetic field spin effect technique was applied. This technique shows that the charge photogeneration mechanism is essentially different in the blends compared to pristine MEH-PPV. Furthermore, photoconductivity in the blends strongly increases compared to pristine MEH-PPV and the photocurrent action spectrum closely follows to the extended absorption tail. We discuss photoinduced charge-transfer and relaxation of photoexcited CTC as possible mechanisms of mobile charge generation.

© 2004 Published by Elsevier B.V.

Keywords: Conjugated polymer; MEH-PPV; Charge-transfer complex; Solar cells; Photoinduced charge transfer; Electron acceptor

Combination of conductivity, optical properties, mechanical flexibility, and ease of processing of conjugated polymers make them promising materials for a number of photonics applications, including large-scale solar cells. In organic photovoltaics, it is essential to provide effective charge generation from the initial photoexcitation. It is generally accepted that photoinduced charge-transfer from a conjugated polymer acting as a donor to an acceptor, for example, a fullerene molecule, is an effective way to generate mobile

charges [1,2]. In the photoinduced charge-transfer process, an exciton photoexcited in the polymer chain diffuses to the donor/acceptor interface and dissociates there into the separate charges. On the other hand, it is possible a more direct way from an incident photon to separate charges using weak charge-transfer complexes (CTCs) of Mulliken type [3]. CTC optical absorption formally implies donor/acceptor electron transfer and as a result a pair of separated charges can be formed. Essentially, as known for short conjugated molecules, the CTC absorption band can be tuned in the region where both the donor and acceptor are transparent [3,4]. This can be used for tailoring low-band gap materials to match

* Corresponding author. Tel.: +7 95 9392228; fax: +7 95 9393113.
E-mail address: paras@polys.phys.msu.su (D.Y. Paraschuk).

the solar spectrum. For example, a weak CTC between C₆₀ and Zn-phthalocyanine molecules was recently reported [5] demonstrating photoconductivity in the near-IR range.

As well known for small aromatic conjugated molecules, they can easily form CTCs in solutions, for example, with a molecule with high-electron affinity. Such CTCs were widely studied in the 50–60 s and their properties were successfully interpreted in the framework of the Mulliken model of CTC interaction [3]. These CTCs usually have characteristic optical absorption in the visible range corresponding to a CTC band. It would be important to obtain a CTC with a conjugated polymer because it would give a possibility to extend the photosensitivity of a conjugated polymer into the red and IR spectral region. At present, there are no reliable evidences of CTCs with conjugated polymers. Blended films of conjugated polymers and organic electronic acceptors, for example, MEH-PPV/C₆₀, MEH-PPV/TCNQ [6], do not usually demonstrate indications of ground-state interaction. Note that early studies of films poly(3-octylthiophene)/C₆₀ showed [7] that their optical absorption spectrum is not just a sum of the donor and acceptor spectra that could indicate CTC. However, the vibrational IR spectra of poly(3-octylthiophene)/C₆₀ did not show any signs of non-additivity [8].

In this work, we tried to realize CTC interaction with long conjugated chains by blending a conjugated polymer with electronegative organic molecules. We studied blends of poly[2-methoxy-5-(2'-ethyl-hexyloxy)-1,4-phenylene vinylene] (MEH-PPV) with 2,4,7-trinitrofluorenone (TNF) or 2,6-dinitroantraquinone (DNAQ) by a number of optical and photoelectric methods. Using optical absorption and FTIR data, we found that in the 1:1 MEH-PPV/TNF and 1:1 MEH-PPV/DNAQ blended films a ground-state CTC can form with essential absorption in the red region. Then, using photoluminescence (PL) and photoinduced absorption (PIA) spectroscopy, we demonstrate that the photoexcited states of MEH-PPV/TNF and MEH-PPV/DNAQ blended films can relax into the charged states. And finally, we show that the photosensitivity of a MEH-PPV/TNF photodiode can be extended into the near-IR spectral range.

1. Experimental

Drop-cast films of pristine MEH-PPV, MEH-PPV/TNF, and MEH-PPV/DNAQ blends were prepared from different solvents (chlorobenzene, toluene, cyclohexanone) with typical MEH-PPV concentration 1 g/l and varying the molar content of the acceptor in the range 1:1000–1:1. For photocurrent and photoconductivity studies, we fabricated single layer diodes in the sandwich structure on ITO-coated glass substrates. A top Al-electrode was deposited on the drop-cast polymer film. The active area of the device was $\approx 0.1 \text{ cm}^2$.

IR vibrational spectra were recorded using a FTIR Analyzer (Simex) in the transmission mode. All spectra were obtained with 2 cm^{-1} resolution and standard window functions at room temperature. FTIR data were recorded mainly

for films prepared by drop-casting on BaF₂ substrates. For PIA spectroscopy studies, the pump beam was mechanically chopped and the PIA signal in the probe channel was processed by a lock-in amplifier at the frequency of modulation. In the probe channel, we used a tungsten-halogen lamp illuminating the sample, a monochromator, and solid-state photodetectors (Si and InGaAs). As a pump source, we used cw Nd:YAG lasers (532, 946 nm), diode lasers (670, 810 nm), and a light emitting diode (630 nm). For pristine MEH-PPV films, the PL was subtracted from the measured PIA signal. The PL and absorption spectra were recorded using the same set-up, the latter were also measured with a spectrophotometer. PIA data were obtained at ambient conditions or under nitrogen flow in the temperature range 100–300 K. To test the effect of oxygen, the room temperature PIA data were also measured in a vacuum cuvette. *I/V* curves of the photodiodes were measured in a vacuum chamber at room temperature using an electrometer (Keithly 617) and a monochromatized radiation of a Xe-lamp. The measurements of the magnetic field spin effect on photoconductivity were performed using this set-up by applying a dc magnetic field with an induction from 0 to 100 mT. The signal compensation scheme was used. Photocurrent spectra were recorded without external bias at ambient conditions using lock-in technique.

2. Results and discussion

2.1. Optical and IR spectra

We found that drop-cast films of MEH-PPV/DNAQ and MEH-PPV/TNF essentially change their color compared with that of pristine MEH-PPV. Fig. 1 shows the absorption spectra of the MEH-PPV/acceptor and pristine MEH-PPV films. It is seen that the absorption spectra of the MEH-PPV/acceptor films are shifted to the red and show extended absorption tails up to 1.5 eV compared with pristine MEH-PPV films. The effect of different solvents for pristine

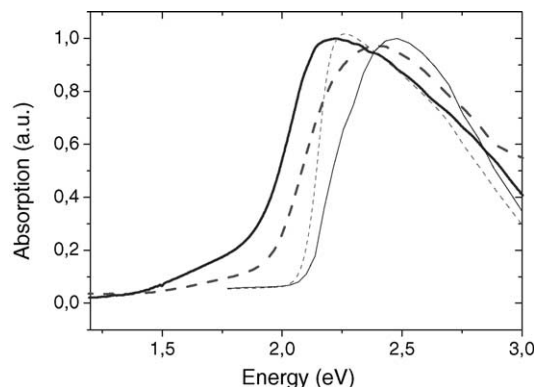


Fig. 1. Normalized absorption spectra of 1:1 MEH-PPV/TNF from cyclohexanone (thick solid); 1:1 MEH-PPV/DNAQ from toluene (thick dashed); pristine MEH-PPV from cyclohexanone (thin solid) and from toluene (thin dashed).

MEH-PPV films is also clearly seen in Fig. 1. Note that light scattering gives negligible contribution to the red absorption tails in Fig. 1 since the prepared films had good optical quality with visually low light scattering. Adding the acceptors did not change the scattering losses implying minor phase segregation. We suggest that the observed features indicate noticeable ground-state interaction of the MEH-PPV chains with the acceptor molecules (DNAQ or TNF), and therefore, CTC formation. In fact, the acceptor electronic absorption bands are in the UV spectral range, and therefore, the spectral features in the range 1.5–2 eV (Fig. 1) we can assign to the CTC bands. On the other hand, MEH-PPV films could show a red shift and an extended absorption tail in other two cases: aggregation of polymer chains or as a result of appearing relatively long-conjugated chains. It is unlikely that either would be the result of blending. In fact, the observed absorption tails in blends are too intensive and red shifted to be assigned to aggregation of polymer chains observed in MEH-PPV [9].

If a CTC forms in a MEH-PPV/acceptor blend, one can expect to observe non-additive lines in the IR absorption spectra associated with ground-state donor/acceptor interaction. FTIR spectra were recorded separately for pristine MEH-PPV, MEH-PPV/acceptor blends, and acceptors (TNF, DNAQ). We found that FTIR spectra of blended MEH-PPV/acceptor films demonstrate non-additive behavior, i.e. the spectra of the blends are not just a superposition of the MEH-PPV and acceptor spectra. The FTIR spectra of MEH-PPV and acceptors are quite rich in the range 800–1500 cm^{-1} and to see the effect of non-additivity clearer, we show in Fig. 2 the FTIR spectrum of a 1:1 MEH-PPV/DNAQ film and a superposition of separately recorded DNAQ and MEH-PPV. The superposition was obtained numerically by multiplying of the MEH-PPV and acceptor spectra with corresponding weights. The superposition reproduces the known lines of MEH-PPV [10] and the characteristic lines of NO₂ groups and anthraquinone [11]. The weight of MEH-PPV was taken according to the intensity of its aliphatic CH bands near 3000 cm^{-1} . The weight of DNAQ was chosen according to the intensity of its characteristic bands and to best fit

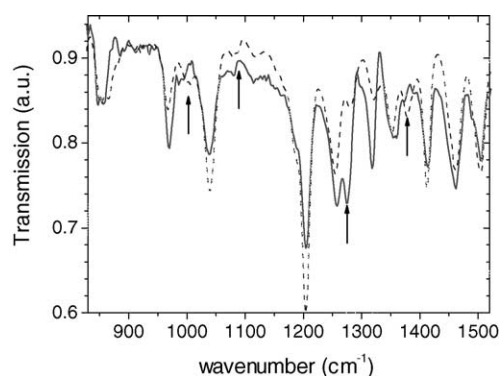


Fig. 2. FTIR spectra of 1:1 MEH-PPV/DNAQ film prepared from chlorobenzene (solid) and superposition of MEH-PPV and DNAQ (dashed). Arrows show the non-additive bands of DNAQ.

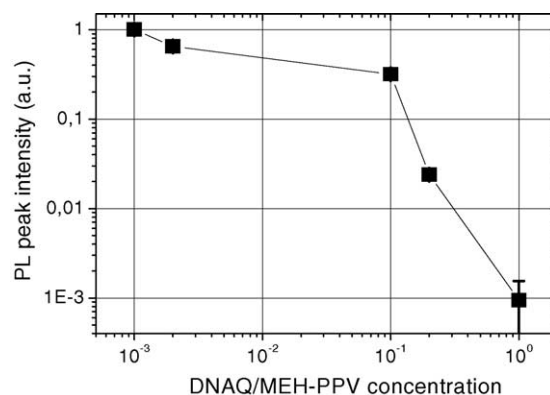


Fig. 3. Peak PL excited at 532 nm vs. molar MEH-PPV/DNAQ concentration for the films prepared from chlorobenzene. The line is a guide to the eye.

to the FTIR spectra of the blend. The arrows in Fig. 2 show the non-additive DNAQ lines which do not overlap with the MEH-PPV lines. Therefore, the FTIR spectrum of MEH-PPV/DNAQ is not a simple superposition of the two components implying noticeable ground-state interaction, which can result from CTC formation between the donor and acceptor.

2.2. Photoluminescence

At the next stage, we studied the properties of the photoexcited states of MEH-PPV/TNF and MEH-PPV/DNAQ films. We found that the PL in MEH-PPV films is strongly quenched upon adding TNF or DNAQ. Fig. 3 shows the peak PL intensity at ~ 600 nm in MEH-PPV/DNAQ films for different acceptor content. It is seen that the PL drops up to 1000 times as the acceptor content increases. The PL shape did not change from that of the pristine MEH-PPV films and only for the highest DNAQ content the PL spectrum was broader and structureless. We associate this effective PL quenching in MEH-PPV/acceptor blends at 532 nm with charge-transfer to the acceptor molecules. In fact, since the absorption spectrum of DNAQ (TNF) does not overlap with the emission spectrum of MEH-PPV, the quenching of the MEH-PPV singlet excitation must be due to electron transfer from the singlet excitation rather than due to energy transfer.

2.3. Photoinduced absorption

We studied MEH-PPV/DNAQ and MEH-PPV/TNF films using PIA spectroscopy. To see the effect of the acceptor, we recorded the PIA spectra of pristine MEH-PPV films as well. Below we present results only for MEH-PPV/TNF films, our results for MEH-PPV/DNAQ films are analogous.

Fig. 4 shows typical PIA spectra for pristine MEH-PPV and MEH-PPV/TNF films at low temperature for photoexcitation in the MEH-PPV absorption band at 532 nm. In pristine MEH-PPV films, the most intensive peak was at 1.35 eV and it is usually assigned to triplet states [12],

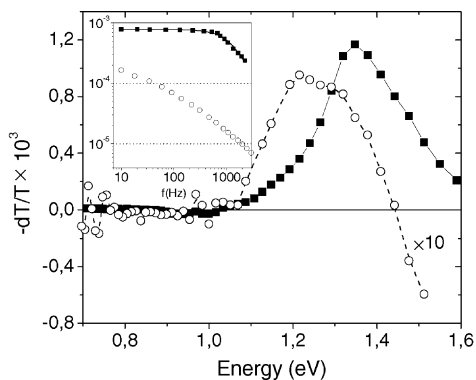


Fig. 4. PIA spectra for pristine MEH-PPV (■) and 1:1 MEH:PPV/TNF (○) films prepared from cyclohexanone at $T=110$ K for pump intensity 100 mW cm^{-2} at 532 nm and chopping frequency 70 Hz. The inset demonstrates the corresponding frequency dependencies of the peak signals at 1.2 and 1.35 eV, the solid line shows a monomolecular kinetics fit for the peak at 1.35 eV.

while in MEH-PPV/TNF blend the PIA spectrum was dominated by the peak at 1.2 eV assigned to charged states (polarons) in MEH-PPV [13]. The different nature of peaks at 1.2 and 1.3 eV is illustrated by their chopping frequency dependences (Fig. 4, inset). Moreover, their temperature dependencies were also essentially different. These observations indicate that in pristine MEH-PPV the PIA at 1.35 eV is associated with triplet excitons and the PIA at 1.2 eV in MEH-PPV/TNF is associated with polarons. Therefore, the MEH-PPV/acceptor films demonstrate photoinduced charge-transfer that is in accordance with the above PL data.

As seen in Fig. 1, the MEH-PPV/acceptor blends have an absorption tail prolonging far to the red region in contrast to pristine MEH-PPV. It is important to find the relaxation pathways of these low-energy excited states, which we assign to CTC states. For this, we studied PIA for red and IR pump radiation with wavelengths corresponding to the observed absorption tail in Fig. 1. Fig. 5 shows PIA spectra for MEH-PPV/TNF and MEH-PPV films at excitation

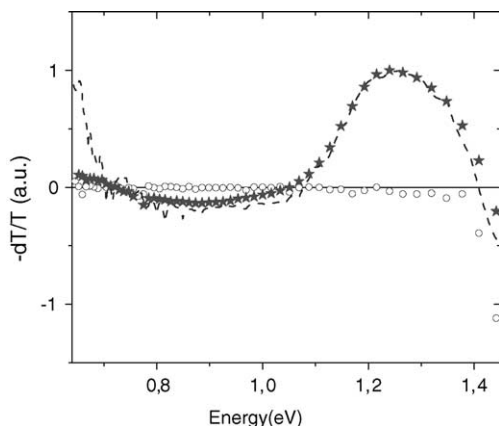


Fig. 5. PIA spectra at 300 K for pristine MEH-PPV (○) and 1:1 MEH-PPV/TNF (★) blend for photoexcitation at 810 nm. The dashed line shows the PIA spectrum of the blend for pump at 532 nm measured in a vacuum cuvette.

wavelength 810 nm at room temperature. The former consists of two polaron bands at ~ 0.7 and 1.2 eV. For pump at 810 nm pristine MEH-PPV films display no PIA signal at all. At the same time, the blend gives nearly the same spectra that were observed for the visible photoexcitation. The similar PIA spectra were obtained for pump wavelengths 629 and 670 nm.

To analyze the photoexcitation efficiency of charged states, the PIA excitation spectrum for the polaron peak at 1.2 eV was measured. We found that the photoexcitation efficiency calculated per absorbed pump photon shows a weak dependence on the excitation wavelength in the range 532–810 nm. Therefore, if we associate the extended red tail in absorption of MEH-PPV/(TNF or DNAQ) films with a CTC, its photoexcitation results in charges states as well as photoexcitation in the main absorption band of MEH-PPV. Thus, in MEH-PPV/acceptor films, we observed photoinduced charge-transfer for photons absorbed by MEH-PPV and relaxation of the CTC into the charged states (polarons) for photons energies corresponding to the CTC band. These results suggest that the sensitivity of plastic solar cells based on appropriate donor/acceptor blends could be extended in the near-IR range where the solar spectrum peaks.

2.4. Photoelectric studies

We fabricated photodiodes with the single working layer of MEH-PPV with various TNF content. Dark I/V curves of the photodiodes demonstrated more rectifying behavior with increasing the TNF content. The rectification ratio was more than 10^3 at ± 1.5 V for 1:1 MEH-PPV/TNF working layer, indicating the characteristic diode behavior. Under illumination the photoconductivity of the MEH-PPV/TNF diodes increased essentially compared with the pristine MEH-PPV diodes.

The magnetic field spin effect (MFSE) on photoconductivity was studied to probe the mechanism of charge generation in pristine MEH-PPV and MEH-PPV/TNF films. In the MSFE, the applied magnetic field exerts influence in particular upon the recombination rate of the geminate electron-hole pairs due to changing the initial singlet state of the pairs [14]. In pristine MEH-PPV films, we observed the photoconductivity change in the applied magnetic field up to 8% for photoexcitation at 500 nm. At the same time, we found that addition of TNF to MEH-PPV led to strong decrease of the MFSE and the MSFE disappeared at very low molar donor/acceptor ratio 100:1. Disappearance of the MSFE indicates that the geminate recombination rate strongly decreased during the lifetime of the coherent spin state of the transient pair ~ 1 ns. Therefore, the disappearance of the MSFE implies charge separation, i.e. fast dissociation of the photoexcited singlet excitons in the MEH-PPV/TNF blends. Thus, the MSFE data correlate with the PIA spectroscopy data indicating that in MEH-PPV/TNF films quite effective charge separation occurs compared with pristine MEH-PPV films.

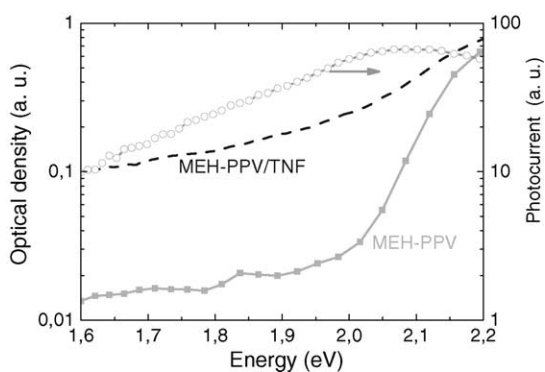


Fig. 6. Photocurrent action spectrum of the 1:1 MEH-PPV/TNF photodiode with thickness of the film ~ 100 nm without external bias and absorption spectra of pristine MEH-PPV and 1:1 MEH-PPV/TNF blend at 300 K. Optical radiation with intensity $\sim 10 \mu\text{W cm}^{-2}$ on the sample was chopped at 120 Hz. The photocurrent spectrum was corrected for the spectral response of the set-up.

Fig. 6 shows the photocurrent action spectrum of a MEH-PPV/TNF photodiode and compares it with the optical absorption spectra of pristine MEH-PPV and MEH-PPV/TNF films. First of all, we are interested in the photocurrent spectra in the red and near-IR regions, where the CTC has considerable absorption (Fig. 1). This spectral region is important from the viewpoint of expansion of the photosensitivity of polymer-based solar cells in the near-IR region. As seen in Fig. 6, in the region of the CTC absorption (600–800 nm), the photocurrent action spectrum closely follows the absorption spectrum of the MEH-PPV/TNF film. Note that the signal for the pristine MEH-PPV films was unobservable. Decreasing of the photocurrent in the absorption peak at 2.2 eV is probably associated with the internal filter effect [15], indicating that the photocurrent generation occurs in the vicinity of the Al-electrode. This implies quite low electron mobility in the acceptor (TNF) network. Thus, in the MEH-PPV/TNF photodiode a qualitatively new feature was observed: photocurrent generation in the spectral region of the CTC absorption.

3. Conclusions

Our data show that a weak CTC is formed between MEH-PPV and TNF or DNAQ with noticeable absorption in the red spectral range. The effect is the most pronounced for

1:1 MEH-PPV/TNF films. We found that photoexcitation in the CTC band can relax into charged states with nearly the same efficiency as for excitation in the main absorption band of MEH-PPV. Moreover, these charged states can relax into mobile charges giving the photocurrent action spectrum well correlated with the absorption spectrum of the blend. Therefore, CTCs based on conjugated polymers can be promising materials for plastic solar cells to extend their sensitivity in the near-IR range.

Acknowledgements

This research was supported by European Office of Aerospace Research and Development via the International Science and Technology Center (Project 2666P) and partly by Russian Foundation for Basic Research (Grant 04-02-16658). We thank A.N. Shchegolkhin for discussion of FTIR spectra.

References

- [1] N.S. Sariciftci, L. Smilowitz, A.J. Heeger, F. Wudl, *Science* 258 (1992) 1474.
- [2] C.J. Brabec, N.S. Sariciftci, J.C. Hummelen, *Adv. Funct. Mater.* 11 (2001) 15.
- [3] R.S. Mulliken, *J. Am. Chem. Soc.* 74 (1952) 811.
- [4] S.P. McGlynn, *Chem. Rev.* 58 (1958) 1113.
- [5] G. Ruani, C. Fontanini, M. Murgia, C. Taliani, *J. Chem. Phys.* 116 (2002) 1713.
- [6] A.J. Heeger, F. Wudl, N.S. Sariciftci, R.A.J. Janssen, N. Martin, *J. Phys. I* 6 (1996) 2151.
- [7] L. Smilowitz, N.S. Sariciftci, R. Wu, C. Gettinger, A.J. Heeger, F. Wudl, *Phys. Rev. B* 47 (1993) 13835.
- [8] K.H. Lee, R.A.J. Janssen, N.S. Sariciftci, A.J. Heeger, *Phys. Rev. B* 49 (1994) 5781.
- [9] T.Q. Nguyen, I.B. Martini, J. Liu, B.J. Schwartz, *J. Phys. Chem. B* 104 (2000) 237.
- [10] K.F. Voss, C.M. Foster, L. Smilowitz, D. Mihailovic, S. Askari, G. Srdanov, Z. Ni, S. Shi, A.J. Heeger, F. Wudl, *Phys. Rev. B* 43 (1991) 5109.
- [11] A. Latef, J.C. Bernede, S. Benhida, *Thin Solid Films* 195 (1991) 289.
- [12] D.S. Ginger, N.C. Greenham, *Phys. Rev. B* 59 (1999) 10622.
- [13] X. Wei, Z.V. Vardeny, N.S. Sariciftci, A.J. Heeger, *Phys. Rev. B* 53 (1996) 2187.
- [14] E.L. Frankevich, *Mol. Cryst. Liq. Cryst.* 324 (1998) 137.
- [15] M.G. Harrison, J. Gruner, G.C.W. Spencer, *Phys. Rev. B* 55 (1997) 7831.